

Cell death induced by application of time-varying magnetic fields on nanoparticle-loaded dendritic cells.

I. Marcos-Campos^{1,2}, L. Asín¹, T. E. Torres^{1,3,4}, C. Marquina^{3,4}, A. Tres^{1,2}, M. R. Ibarra^{1,3,4} and G. F. Goya^{1,3,†},

¹ *Instituto de Nanociencia de Aragón (INA), University of Zaragoza, Pedro Cerbuna 12, 50009- Zaragoza, Spain.*

² *Oncology Department, Hospital Universitario “Lozano Blesa”, 50009 Zaragoza, Spain.*

³ *Condensed Matter Department, Sciences Faculty, University of Zaragoza, Spain 50009.*

⁴ *Instituto de Ciencia de Materiales de Aragón (ICMA), CSIC-Universidad de Zaragoza, 50009 Zaragoza, Spain*

† *Corresponding author: goya@unizar.es.*

Instituto de Nanociencia de Aragón (INA), University of Zaragoza, Pedro Cerbuna 12, 50009- Zaragoza, Spain.

Tel.: +34 976 762777

Fac.: +34 976 762776.

Abstract.

Aim: To assess the capability of monocyte-derived dendritic cells (DCs) to take Fe₃O₄ magnetic nanoparticles (MNPs), keeping their viability. To provoke cell death on these MNPs-loaded DCs using an external alternating magnetic field (AMF). **Material & methods:** Peripheral blood mononuclear cells were isolated from normal blood and platelets removed by centrifugation. Immunoselected CD14⁺ cells were cultured for 5 days, and the resulting cell phenotype was determined against several markers using flow cytometry. Co-cultures of DCs and MNPs were done overnight. The amount of Fe₃O₄ nanoparticles incorporated by DCs was quantified by magnetization measurements. MNPs-loaded DCs were exposed to AMF for 30 min and then cell viability was measured using trypan blue and FACS (annexin-propidium iodide) protocols. Morphological changes were investigated using scanning electron microscopy. **Results:** No significant decrease in cell viability of MNP-loaded DCs was observed up to five days, as compared against control samples. The power absorption experiments in AMF showed that only magnetically-loaded cells were killed when exposed to the magnetic field, yielding ca. 95% of cell death. However, we found that the amount of incorporated magnetic material within the cytoplasm (1 to 5 pg/cell) was unable to raise the temperature of the cell culture. **Conclusion:** Our results point to local damage produced by the MNPs as the main mechanism for the selective cell death of MNP-loaded DCs under AMF. Based on the ability of these cells to evade the reticuloendothelial system, these complexes in combination with AMF should be considered as a potentially powerful tool for tumor therapy.

Abbreviations: Hyperthermia (H); Dendritic Cells (DCs); Magnetic Nanoparticles (MNPs).

Keywords: Dendritic cells, magnetic nanoparticles, magnetic hyperthermia; cell viability, tumor targeting.

Introduction

Dendritic cells (DCs) are the most important antigen-presenting cells (APC), with a key role at the first steps of most immune responses. [1] The main hallmarks of DCs are their high potential to capture, process and present antigens through MHC-I and MHC-II molecules to T cells. DCs are derived from bone marrow precursors and migrate to non-lymphoid tissues where they differentiate into dendritic cells.[2] The process of activation of DCs occurs in two stages. DCs reside in peripheral tissues as immature DCs, characterized by a high capacity to capture antigens, and undergo a maturation process due to stimuli originated by pathogens or apoptotic cells.[3] Once DCs are in the mature state, they change the molecular expression pattern in their membrane and migrate to lymph nodes, [4] where the antigen presentation to T cells takes place. It is well known that DCs can be differentiated from monocytes *in vitro* in the presence of GM-CSF and IL-4. This ability of differentiating DCs *in vitro* has settled the first step for future applications as therapeutic agents in several diseases. [5]

The increasing synergy between biomedicine and nanoscience has its paradigm in the use of magnetic nanoparticles (MNPs) in routine laboratory and clinical protocols, such as cell sorting, DNA separation, Magnetic Resonance Imaging (MRI) and gene therapy. [6, 7] Applications of MNPs currently in preclinical stages include cell-targeted delivery of anticancer agents and molecular diagnosis. [8, 9] Very recently, magnetic hyperthermia trials have passed preclinical stages and received regulatory approval as clinical protocol for thermotherapy.[101] For the medium-term future, it is envisaged that with proper control of size and surface functionalization

these MNPs could be used as multifunctional intracellular agents for MRI, drug carriers and/or heat generators for hyperthermia. [10]

Loading MNPs with anticancer drugs and targeting them to specific tumor sites is a promising strategy for detection and elimination of neoplastic cells disregarding their physical size, which in turn could stop metastatic cells from proliferating. A major obstacle for this approach is that the reticuloendothelial system is a very effective system that detects and phagocytoses MNPs, preventing their therapeutic function.[11] Currently, the main strategy for evading the RES is based in NP-functionalization approaches, intended to mimic biologic entities already present in the blood system and transform the MNPs in 'stealth' carriers.[12] On the other hand, eukaryotic cells can be easily 'targeted' *in vitro* with NPs because the dimensions of the latter are comparable to subcellular structures. Depending on the kind of core materials and surface charge employed, different mechanisms for detecting and/or uptaking inorganic nanoparticles have been observed, but the general consensus is that particle incorporation is strongly dependent on the cell type involved.[13]

Being antigen-presenting cells, DCs are quite active at the membrane level and thus good candidates to incorporate MNPs. Uptake of different antigens by DCs occurs by differentiated processes such as macropinocytosis, phagocytosis or receptor-mediated endocytosis [14] and indeed several works have demonstrated that DCs can uptake peptides, viral RNA, bacterial DNA and other molecules. [15]. Moreover, it has been also described the ability of DCs to incorporate several kinds of solid particles within a broad size range [16].

In the presence of proangiogenic factors, DCs can transdifferentiate into cells with a similar phenotype and functionality of endothelial cells (*endothelial-like cells*,

ELCs) and contributes to the formation of new vessels by vasculogenesis [17, 18]. Tumor needs a vessel network which provides it oxygen and allows its growth. It is well known that tumoral cells need an increased oxygen supply with respect to normal cells, and for this purpose tumors growth is often accompanied by fast vasculature growth. [19] It has also been reported that several cell types are ‘recruited’ by the tumor to accelerate the formation of new blood vessels, both endothelial cells and circulating cells, in a process called angiogenesis [20, 21].

In the present work, we show the first results on a new strategy, based on the use of dendritic cells as natural carriers of MNPs to the desired target tissue. The bottom line of using dendritic cells as carriers of MNPs is to mimic biological units in order to elude the immune response of the body. The potential of this strategy is that the cargo of the DCs could be designed to be either ‘nude’ magnetic MNPs for hyperthermia therapy, or functionalized MNPs with specific drugs that could be released by application of time-varying magnetic fields. This work has two major goals: a) to study the inclusion and toxicity effect of magnetic nanoparticles on dendritic cells; and b) to induce cell death by applying a time-varying magnetic field on the NP-loaded DCs. We also present an easy method to quantify the incorporation of MNPs into DCs, based on magnetization measurements, which has the potential to quantify the amount of magnetic material absorbed.

Materials and Methods

a. Magnetic Nanoparticles

Two different types of MNPs were selected from a larger set of 18 different types of magnetic colloids commercially available (*Micromod GmbH, Germany*)

[102], having different surface functional groups and magnetic core sizes (see Figure 1). All MNPs evaluated were composed of a magnetite core (Fe_3O_4) with average sizes between ca. 8 and 16 nm, and a dextran shell at the surface. The selection of the two types of colloids for this work was based on their ability to generate heat when submitted to alternate magnetic fields, because the final purpose was to perform magnetic hyperthermia experiments.

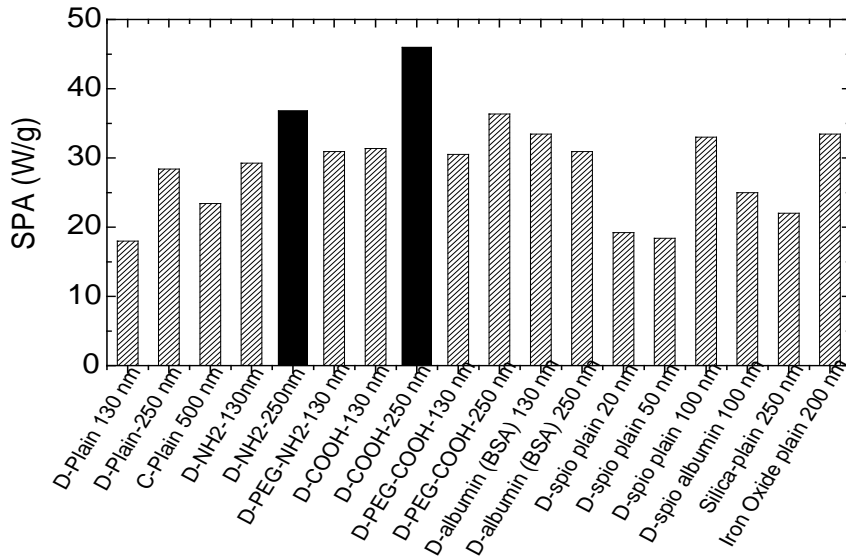


Figure 1: Specific Power Absorption (SPA) measured for a series of commercial water-based colloids with nanoparticles having different core sizes and surface functional groups. The solid bars represent the two types of colloids selected for the experiments.

Among those colloids having the largest Specific Power Absorption (SPA) values, we selected two samples with the same hydrodynamic radius and opposite surface charge (the filled bars in Figure 1), in order to check the effect of surface charge on the upload affinity of the cells. Samples with MNPs positively charged (by amine groups at the surface, NH_2^+) and those negatively charged (carboxyl groups COOH^- at the surface) were labeled as MCM+ and MCM-, respectively. In addition to the specifications from the provider [22] the nanoparticles were characterized through

Transmission Electron Microscopy (TEM), Dynamic Light Scattering (DLS), and magnetization measurements.

The magnetic characterization of both colloids and cell cultures was performed in a commercial SQUID magnetometer (Quantum Design MPMS-XL), through static measurements as a function field and temperature. Pure colloids and cell cultures were measured *as is*, i.e. in liquid phase, after conditioned in sealed sample holders of 200 μL capacity. Magnetization data was collected in applied magnetic fields up to 5 T, between 5 K and 250 K to avoid the melting of the frozen liquid carrier of colloids and the cell support (culture media). To check the magnetic behavior at room temperature, hysteresis loops $M(H)$ were performed at $T=295$ K in samples previously dried at room temperature.

b. Dendritic cells differentiation from PBMCs

Peripheral blood mononuclear cells (PBMCs) were isolated from normal blood by density gradient (*Ficoll Histopaque-1077, Sigma*). Cells were washed twice with PBS for 7 minutes at 1200 rpm at room temperature. To avoid platelet contamination, cells were centrifuged 10 minutes at 800 rpm. CD14⁺ cells were isolated with magnetic beads (*CD14 Microbeads, Miltenyi*) by positive immunoselection using the autoMACS Separator (Miltenyi) as described by the manufacturer.

In T75 flask, CD14⁺ positive cells (10^6 cells/ml) were cultured in RPMI 1640 (*Sigma*) with 10% FBS, 1% glutamine, 1% antibiotics (100 U/ml penicillin and 100 ng/ml streptomycin) and supplemented with IL-4 (25 ng/ml) and GM-CSF (25 ng/ml)(*Bionova*). Cells were cultured for 5 days at 37°C with 5% CO₂ in a humidified atmosphere. Every second day, medium was replaced by fresh medium containing the same concentration of interleukins. Dendritic cells phenotype was characterized by

staining with fluorochrome-labelled antibodies against CD45, CD14 (BD Biosciences, San Jose, CA), CD11c (eBioscience, San Diego, CA), HLA-DR, CD40, CD80, CD83 and CD86 (Invitrogen, Carlsbad, CA) and DC-SIGN. Flow cytometry analysis was performed with the FACScalibur cytometer and data was analyzed with the FACSDiva software.

c. Cytotoxicity assay

On the fifth day of the differentiation process, loosely adherent and non-adherent cells were collected from the T75 flask. Cells were washed twice and seeded onto a 6-wells plate at 10^6 cells/ml in complete medium supplemented with IL-4 (25 ng/ml) and GM-CSF (25 ng/ml). The cytotoxicity of both MCM- and MCM+ colloids (with nominal concentration of 10 mg Fe_3O_4 /ml) was evaluated by adding 5 μl /ml media in three wells each, and cell viability was measured on days 1, 3 and 5 after MNPs addition by trypan blue, MTT test and FACS using annexin-propidium iodide markers. Trypan blue assay was carried on by diluting 10 μl of cells sample in trypan blue (1:1). A drop of the cells and trypan blue mixture was placed in a hemacytometer. Cells were counted in an optical microscopy differentiating those that were stained in blue (death cells) and those unstained (live cells).

For MTT cell viability assay, 2.5×10^5 dendritic cells were taken from each sample and incubated with 20 μL 5 mg/ml MTT for 2 hours in Eppendorf tubes at 37°C in CO_2 incubator. The resultant formazan crystals were dissolved in 200 μL dimethyl sulfoxide and the samples were spun down to remove the cellular debris and nanoparticles, which can act as interference. 100 μl of each sample were placed in a 96-well plate and the absorbance was measured by an ELISA reader at 550 nm. The

percent viability was calculated as: (absorbance treated cells/ absorbance untreated cells) x100. Each assay was repeated three times.

DCs viability was also measured by flow cytometry using a commercial kit (Immunostep, Spain). Briefly, 10^6 cells of each sample were resuspended in Annexin-binding buffer and stained with 5 μ l of the Annexin and 5 μ l of propidium iodide. DCs were incubated for 15 minutes in the dark at room temperature. Cells analysis was performed using the FACS Aria Cytometer and the FACSDiva Software.

d. Morphological Analysis by Scanning Electron Microscopy

We investigated possible effects of the ac magnetic fields on the cell morphology by scanning electron microscopy (SEM). Images were taken of those NP-loaded cell samples with and without hyperthermia protocols. The samples were prepared by fixing the cells with 2.5% glutaraldehyde in 0,1M sodium cacodylate 3% sucrose solution for an hour and a half at 37°C. Dehydration process was carried out by incubating with rising concentrations of methanol: 30, 50, 70, and 100%, each of them for 5 minutes twice and finally anhydride methanol for 10 minutes. A drop of each sample was placed onto a coverslide and wait to be air-dried. Samples were then sputter-coated with gold and examined in a FEI INSPECT F scanning electron microscope, with accelerating voltage of 30kV. Energy-dispersive x-ray spectroscopy was performed using an EDX analyzer system INCA PentaFETx3, with energy resolution range between 137 eV to 5.9 keV.

e. Specific Power Absorption experiments

Specific power absorption (SPA) of the pure colloids was measured with a commercial ac field applicator (model DM100 by nB nanoscale Biomagnetics, Spain)

working at $f = 260$ kHz and field amplitudes from 0 to 16 mT, and equipped with an adiabatic sample space (~ 0.5 ml) for measurements in liquid phase. For *in vitro* magnetic hyperthermia experiments, DCs cultured as described above were collected on day 5 and seeded onto a 6-wells plate at 10^6 cells/ml in complete medium supplemented with IL-4 (25 ng/ml) and GM-CSF (25 ng/ml). A concentration of 5 μ l/ml medium of MCM- and MCM+ nanoparticles suspension (1% wt.) were added in two wells each. Two wells without nanoparticles were used as a control. Cells were cultured overnight at 37°C. Next day, non adherent cells were collected from each well and washed four times with fresh medium to remove the non incorporated NPs. Cells were counted and resuspended in 500 μ l of complete medium.

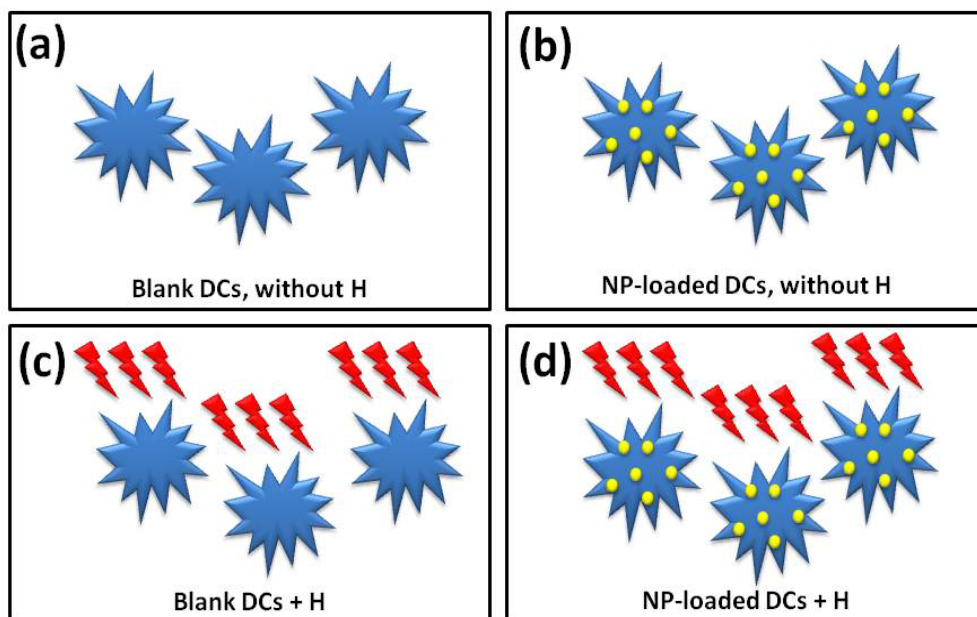


Figure 2: Scheme of the ‘2x2’ experiment: (a) DCs without neither MNPs uptake nor magnetic field application. (b) DCs uptaken with MNPs but without field application, (c) DCs without MNPs for magnetic field application, and (d) DCs with MNPs and application of magnetic fields.

Each experiment comprised four samples of cultured DCs, as illustrated in Figure 2. In this type of ‘2x2 experiment’, the first pair of samples consisting of *as*

cultured blank DCs (i.e., without nanoparticles, Fig. 2a) and NP-loaded DCs (Fig. 2b), were not exposed to magnetic fields and analyzed at the end of the experiment in order to compare the natural viability of the cell culture. The second pair of samples, blank and NP-loaded DCs (Fig. 2 c and d), were exposed to the alternating magnetic field (260 kHz and H=16 mT) for 30 minutes, while measuring the medium temperature. After the field exposure, cell viability was measured in the four samples, using trypan blue and FACS (annexin-propidium iodide) protocols as described previously.

Results and discussion

Optimizing the uptake of MNPs by the DCs is the first step before these cells can be used as carriers to tumoral vasculature.[23] Endocytosis is perhaps the most common among passive mechanisms for MNPs uptake by different cellular types, including HeLa, fibroblasts and DCs. Several previous studies have reported on the uptake of different complexes by the cell, or the inclusion of latex-type nanospheres [24, 25], proposing also models for the mechanisms of phagocytosis. Many works have described the potential of DCs to incorporate a wide range of antigens and molecules [26, 27], and our previous work showed that monocyte-derived DCs are also able to incorporate MNPs into cytoplasmatic compartments[28]. In many cell lines the uptake of MNPs occurs in a concentration and time dependent manner[29] that depends on some specific features of the MNPs involved. In the absence of MNPs surface functionalization with specific biologic ligands, the most probable method to incorporate these MNPs is the unspecific endocytosis

a. Magnetic nanoparticles

Figure 3 shows a typical TEM image of the colloids used in this work. As a general feature, we observed cubic-rounded shapes of the magnetic cores, with some degree of agglomeration even after strong ultrasonic process and high dilutions. Therefore the presence of agglomerates in the colloidal suspension cannot be discarded. The average size of the magnetic cores was obtained after counting > 100 nuclei from different images, and fitting the resulted histogram with a log-normal function. This shape was chosen after finding in both samples a significant fraction of large, cubic-shaped particles. The resulting diameters were $\langle d \rangle = 13 \pm 2$ and 15 ± 2 nm, and the dispersion values $\sigma = 0.5$ and 0.6 for samples MCM+ and MCM-, respectively

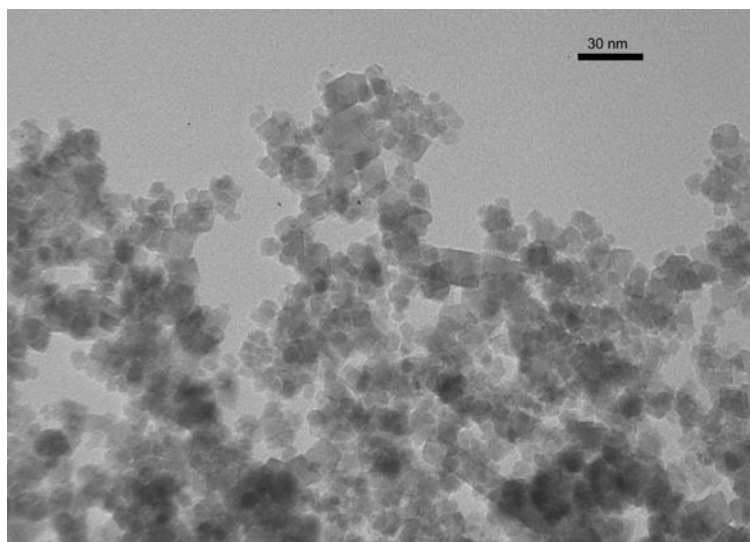


Figure 3: TEM image of Fe_3O_4 nanoparticles with magnetic cores of $\langle d \rangle = 13(2)$ nm, functionalized with NH_2^+ groups at the surface.

The hydrodynamic diameters of the colloidal nanoparticles were extracted from the DLS curves at room temperature. Both MCM+ and MCM- samples displayed a log-normal profile (Figure 4) with a broad peak at ca. 240 nm, and a ‘tail’ to larger particle sizes. The large value of d_H (≈ 18 times the size of the magnetic core) exemplifies the importance of the organic coating for biomedical applications, since

particle aggregates close to the micrometer range should be difficult to incorporate by usual endocytosis mechanisms. Since DLS measurements are performed on highly diluted colloids, the observed dispersion for particle sizes ($\sigma_H = 0.40-0.50$ values of the fitting log-normal function) reflects the presence of cluster units in the colloid, in agreement with the agglomeration observed in TEM images discussed above.

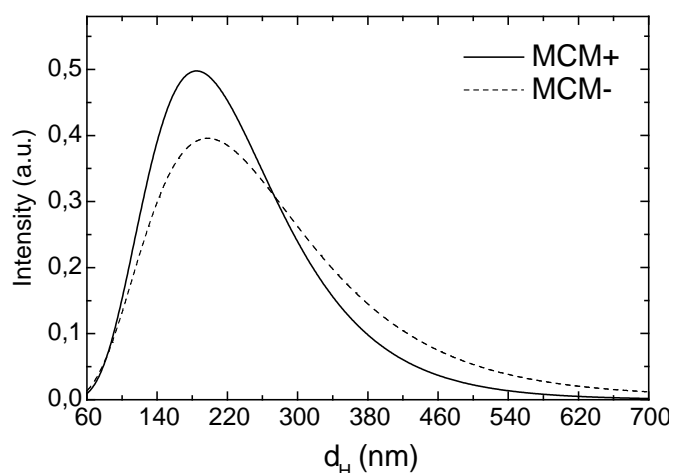


Figure 4. DLS results for the MCM+ (solid line) and MCM- (dashed line) nanoparticles.

The different types of nanoparticles listed in Figure 1 displayed some variation of their Specific Power Absorption values. This is consistent with the different sizes of their magnetic cores (from 5 to 16 nm), since the power absorption is known to depend strongly on particle size.[30] Indeed, there is usually a narrow size window at which the SPA is optimum, centered at some size value that depends on the saturation magnetization and magnetic anisotropy of the core material. The two samples chosen in this work, with opposite surface charge, showed the highest SPA values: 36,8 W/g and 46 W/g for MCM+ and MCM- samples, respectively.

The $M(T)$ curves taken in ZFC and FC modes, for both MCM+ and MCM- samples showed similar behavior, reflecting the similar size and composition of the magnetic cores of both samples. The continuous increase of the $M(T)$ data taken in ZFC mode (Figure 5) suggests that the blocking temperature T_B is near above the maximum measuring temperature. The single-domain nature of the particles is inferred also from the absence of the jump in $M(T)$ curves in ZFC mode, expected for the Verwey transition in multidoman particles.[31-33] In agreement with the proximity of the T_B inferred from $M(T)$ data, hysteresis loops $M(H)$ performed at 295 K in lyophilized colloids showed nearly zero coercive field H_C (see Figure 5), supporting the picture of single domain nanoparticles in the superparamagnetic regime. The magnetic parameters extracted from the $M(H)$ curves at low temperatures (not shown) indicated a slightly reduced M_S , as frequently found in <10 nm Fe_3O_4 particles and attributed to surface spin disorder. [31] The relevant magnetic parameters are summarized in Table I.

Table I: Chemical and physical parameters of the nanoparticles used in this work, surface functional groups, core size d_{CORE} , hydrodynamic size (d_H) and distribution (σ_H), saturation magnetization (M_S), coercive fields H_C and specific power absorption (SPA) values.

Sample	Core material	Surface charge	d_{CORE} (nm)	d_H (nm)	σ_H	M_S (emu/g)	H_C (Oe)	SPA (W/g)
MCM+	Fe_3O_4	NH_2^+	13(2)	244(2)	0.48	62.3	12(5)	36(6)
MCM-	Fe_3O_4	$COOH^-$	15(2)	217(2)	0.43	68.0	12(5)	46(6)

In summary, the observed magnetic behavior is consistent with a single-domain structure of the NPs core, in agreement with previous results on similar Fe_3O_4 NPs within this size window.[31, 33] This is a requisite for effective energy absorption through Néel relaxation mechanisms.

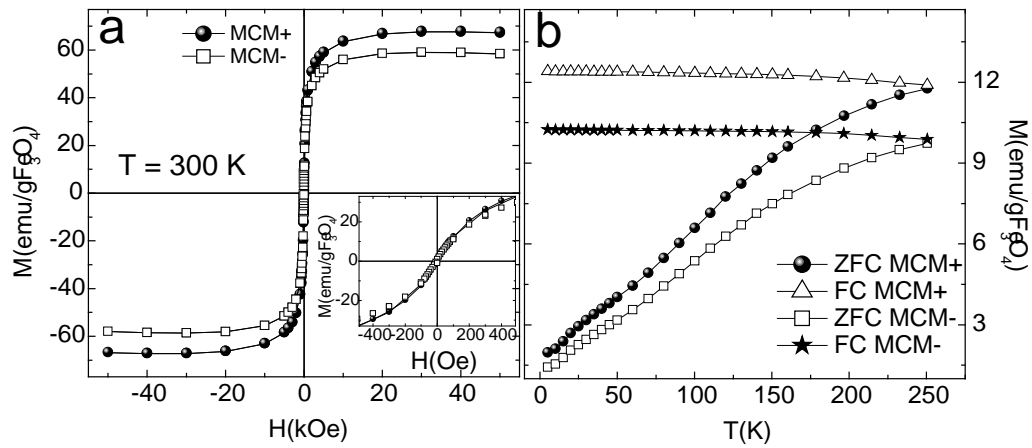


Figure 5: Magnetic data from magnetic colloids used in this work. a) Hysteresis loops $M(H)$ at room temperature. The inset show the small coercive field; b) ZFC-FC data for the same colloids, showing the single-domain behavior with blocking temperatures above 250 K.

b. Dendritic cells differentiation from PBMCs

Monocytes (CD14+) cultured for 5 days in the presence of GM-CSF and IL-4 shown the characteristic phenotype of immature DCs. As shown in Figure 6, the expression of the main markers characterizing immature DCs was confirmed: CD45 (a leukocyte common antigen); CD40 (a common feature of TNF receptor family members which play an important role in DCs maturation) and CD11c (a transmembrane protein present at high levels on most human DCs). Additionally, we verified the absence of specific markers such as CD14 (which is expressed by monocytes that differentiate into DCs but not expressed in DCs themselves); and also the lack of CD83 and CD86 expression (typically absent for immature DCs but present after maturation). These results (both positive and negative) combined are in agreement with a phenotype of immature DCs.

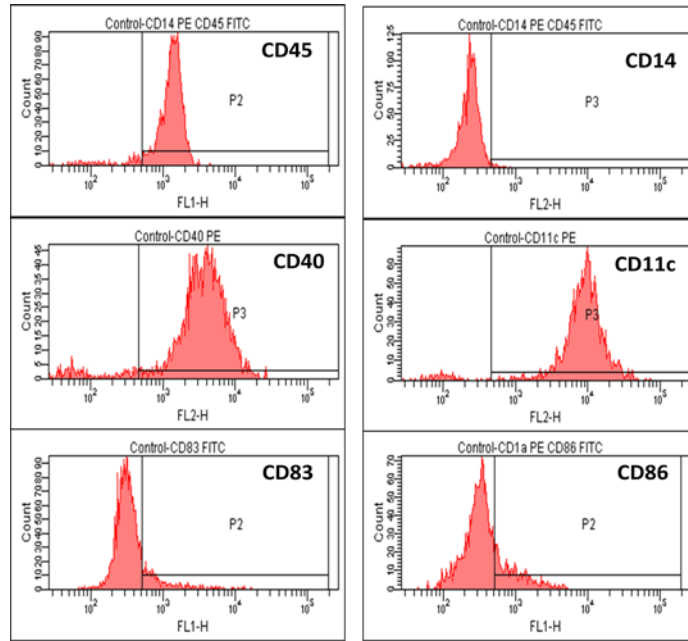


Figure 6: Surface antigen expression measured by FACS for 5 day-cultured cells. The labels in each figure denote the type of FITC or PE-conjugated antibodies used in each case. The resulted phenotype is the immature DCs one.

c. Cytotoxicity assay

The cytotoxicity of the MNPs was checked by trypan blue, flow cytometry and MTT analyses. The main results, presented in Figure 7, show that the viability of DCs after 1, 3 and 5 days of co-culturing with both MCM+ and MCM- decreased in a similar trend than the control sample (without MNPs), remaining above 65-70% in all cases. As the cell culture is a primary one is normal to observe cell death growth through time. Flow cytometry and MTT assays corroborate Trypan blue results as can be seen in the dot-blot representations of flow cytometry data that correspond to DCs after 3 days of incubation with the two different types of MNPs that show cell viability about 90%. (Rest of data not shown)

This similar trend of MNP-loaded and blank DCs, confirmed with three different methods, shows that no major cytotoxic effects can be attributed to the MNPs at the concentration and times of incubation used in this work.

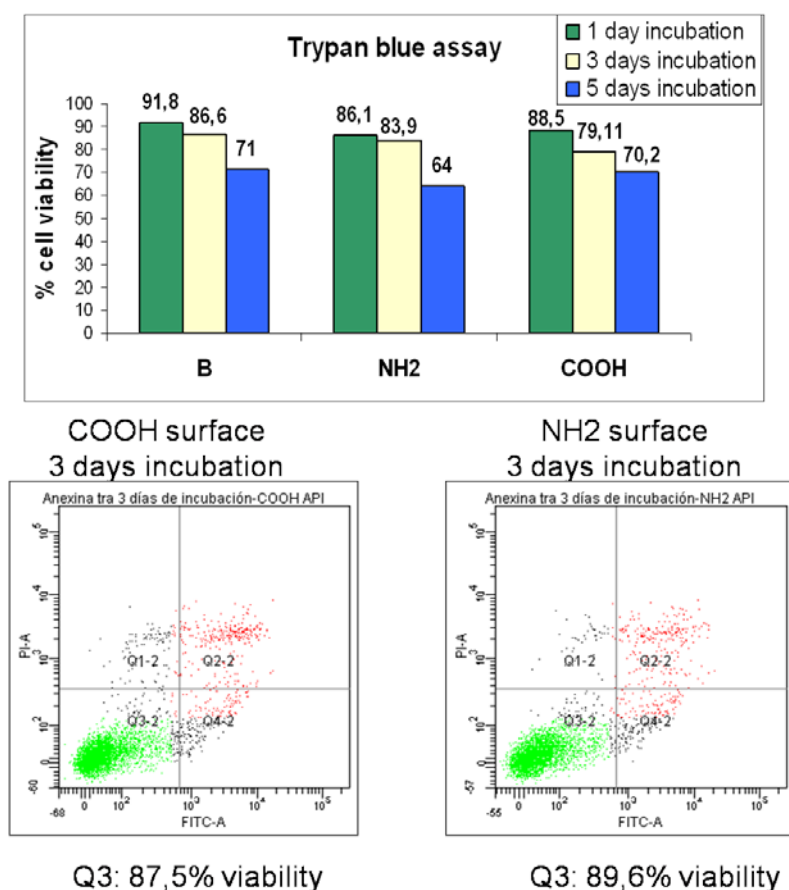


Figure 7: Cell viability verified for COOH and NH₂⁺ surface charge of the MNPs. It can be seen that nearly 90% of the original cells remained viable after 3 day incubation with MNPs. The three methods showed agreement within experimental error.

Cytotoxicity produced by MNPs is one of the main aspects to overcome for biomedical applications. Polystyrene particles have been widely used for this purpose because they are commercially available with different fluorescent markers; surface charge and well defined sizes from few nanometers to few microns. Using these kind of particles it has been demonstrated that cytotoxic effects depend on both size and surface charge.[34, 35] Also, functionality of DCs should be preserved in order to use

them as effective carriers to vascular targets. Therefore our first step to evaluate the actual potential of this strategy was to verify whether DCs can incorporate this kind of MNPs without affect their viability. In a previous work, Wang et al. have studied the uptake of multiwalled carbon nanotubes (CNT) by immature dendritic cells (iDCs), finding that the incorporation of CNTs does not induce phenotypical changes in iDCs, neither affects the normal activation by LPS.[36] At the cellular level, our results demonstrate that both types of NPs used (with COOH^- and NH_2^+ functionalized surfaces) did not significantly alter DCs viability after five days, at the concentrations used in this work. It should be noted that in the case of MCM-, incorporation by DCs was only slightly higher than with MCM+, as inferred from magnetic measurement of the MNPs-loaded DCs cells (see below). However, the lack of differences in cell viability between DCs loaded with MCM- and those loaded with MCM+ suggests that the superficial charge affects neither the cell uptake mechanism nor viability.

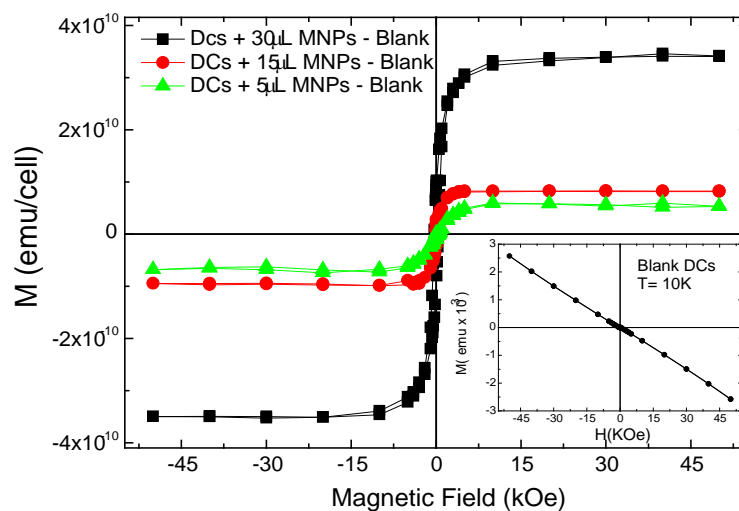


Figure 8: Magnetic signal from DCs cultivated overnight with 30 $\mu\text{L}/\text{mL}$ medium (squares); 15 $\mu\text{L}/\text{mL}$ medium (circles) and 5 $\mu\text{L}/\text{mL}$ medium (triangles) of MCM- nanoparticles. The diamagnetic signals of blank DCs (inset) have been subtracted in all cases.

d. Quantification of uploaded MNPs

Magnetic measurements on the MNP-loaded DCs were performed as a simple way of quantifying the amounts of magnetic material incorporated. For these experiments, several wells of DCs were cultured 12 h with increasing concentrations of MNPs, and afterwards washed several times to eliminate non-incorporated MNPs. Cells were then centrifuged and the obtained pellet conditioned in closed containers for magnetic measurements. A control culture (i.e., without NPs) was measured at the same temperature in order to subtract the strong diamagnetic signal from the DCs at low temperatures (see inset in Figure 8). All measurements were done using 10^6 cells. The $M(H)$ curves obtained at $T = 10$ K (Figure 8) showed a gradual increase in the ferromagnetic signal, indicating an increasing amount of magnetic material incorporated by the cells. Using the M_s values of the pure ferrofluid and the average volume of the magnetic cores extracted from TEM images, we were able to determine the average number of NPs per cell, obtaining from 1×10^4 to 7×10^4 NPs/cell. This relatively small number of particles is able to induce cellular death when submitted to alternate magnetic fields, as will be discussed in the next section. In a previous work on the intracellular distribution of Fe@C nanoparticles on dendritic cells[28], it has been demonstrated using TEM images that the NPs are located within cytoplasmatic organelles, where MNPs aggregates forming >200 nm size structures.

In order to study the physical state of aggregation of the NPS at the intracellular space, we have analyzed the magnetic state of the NPs at room temperature in samples of DCs+NPs, previously lyophilized. Similarly to the pure colloids at room temperature (Figure 5), the particles uploaded by the cells also displayed SPM behavior reflected in the $M(H)$ curves with null coercivity at 300 K. The magnetization of such particles in the SPM state is described by the expression

$M=M_S L(x)$, where M_S is the saturation magnetization and $L(x)$ is the Langevin function with $x=\mu H/k_B T$, where μ is the magnetic moment of a single MNP, H the applied field, k_B the Boltzmann constant and T the temperature. To take account of the volume distribution, the SPM magnetization of the particles is better described as a weighted sum of Langevin functions[31]

$$M = \int_0^{\infty} L \left[\frac{\mu(V)H}{k_B T} \right] f(V) dV \quad (1)$$

Where $f(V)$ represents the distribution function of the particle volume, usually assumed as a log-normal function. It should be noted here that this expression assumes that the system is comprised of *noninteracting* particles. The fit of $M(H)$ curves at room temperature using Eq. (1) (not shown) of a) *as prepared* ferrofluid and b) magnetically loaded DCs resulted in identical fitted parameters within error, indicating that a) the Fe_3O_4 phase is not reduced/oxidized in the intracellular medium and b) the particle size distribution remains essentially unaltered after the incorporation into DCs (i.e., no selective sizes are incorporated). Moreover, as in previous works TEM images showed that MNPs are agglomerated inside the lysosomal/endosomal spaces[28], we conclude that the dextran/functionalized shell is thick enough to prevent strong interparticle interactions. This is an important issue regarding heating experiments *in vitro*, since strong interacting NPs could result in a decrease of the power absorption.

e. Power absorption experiments

Once the incorporation of NPs was verified and cytotoxicity evaluated, we started to study the effects of alternating magnetic fields on NP-loaded DCs. The heating efficiency of the magnetic colloids was measured through the absorbed power

P divided by the mass m_{NP} of the constituent nanoparticles diluted in a mass m_{LIQ} of liquid carrier. The expression for the Specific Power Absorption can be written as [10]

$$\Pi = \frac{P}{m_{NP}} = \frac{m_{LIQ} c_{LIQ} + m_{NP} c_{NP}}{m_{NP}} \left(\frac{\Delta T}{\Delta t} \right), \quad (2)$$

where c_{LIQ} and c_{NP} are the specific heat capacities of the liquid carrier. Since the concentrations of MNPs are usually in the range of 1 % wt., we can approximate [30] $m_{LIQ} c_{LIQ} + m_{NP} c_{NP} \approx m_{LIQ} c_{LIQ}$ and (2) can be written as

$$\Pi = \frac{c_{LIQ} \delta_{LIQ}}{\phi} \left(\frac{\Delta T}{\Delta t} \right), \quad (3)$$

with δ_{LIQ} and ϕ are the density of the liquid and the weight concentration of the MNPs in the colloid, respectively. The conversion from magnetic field energy into heat by the absorbing elements (i.e., the magnetic nanoparticles) at the frequencies of the experiment is due to Néel relaxation process. Many recent works have studied the details of this mechanism that involves heat transference from nanoscopic agents (MNPs) to the macroscopic scale of the colloid, and the common output is that there is a strong dependence between SPA and particle size, with a narrow peak of absorption near the single- to multi-domain transition.[37, 38] Being a heat transference mechanism, an *adiabatic* experiment is needed in order to obtain the actual SPA values for a given material by measuring the exact energy released as a temperature increase within the sample. Since heating of a macroscopic amount of sample takes 10^2 to 10^3 seconds, high insulation is needed in order to grant adiabatic conditions

during the whole experiment. Complete insulation is seldom attained in hyperthermia experiments [39], as can be inferred from the sudden decrease of temperature when the field is turned off. This condition hinders the accurate determination of the final temperature that could be attained with a given set of nanoparticles. However, our criterion for choosing a representative SPA value is related to the maximum slope of the T vs. time curves, which occurs at the first seconds of the experiments. In this way we can ensure that the system behaves adiabatically, since the amount of heat lost during a few seconds interval can be neglected. On the other side, *in vitro* and *in vivo* power-absorption experiments are performed in strong heat exchange conditions and therefore it is neither possible nor interesting to quantify the power absorbed by the MNPs or the cells. Although in hyperthermia experiments the measured parameter is the temperature increase of the cellular culture, the resulting cellular damage has to be related to the actual intracellular temperatures attained within the cytoplasm and/or the nucleus. However, to the best of our knowledge, there are not yet detailed studies on the dynamics of heat conduction from the intracellular medium through the cell membrane.

As described in the experimental section, DCs cultures were always conducted in parallel wells (i.e. two wells for both blank and NP-loaded DCs), in order to compare their viability in cells that were submitted to rf fields and those that were not. The results of these experiments can be seen in Figure 9, from which cell viability obtained from FACS was observed to remain on the $\approx 87-93\%$ level for samples a, b, c and e. On the other hand, the application of the magnetic field on NP-charged DCs resulted in a sharp decrease to 2-5 % of cell viability (Figure 9.e), demonstrating the efficacy of rf magnetic fields for killing targeted cells. Data from trypan blue viability

analysis (not shown) confirmed these results regarding viability of targeted DCs with and without application of rf magnetic field.

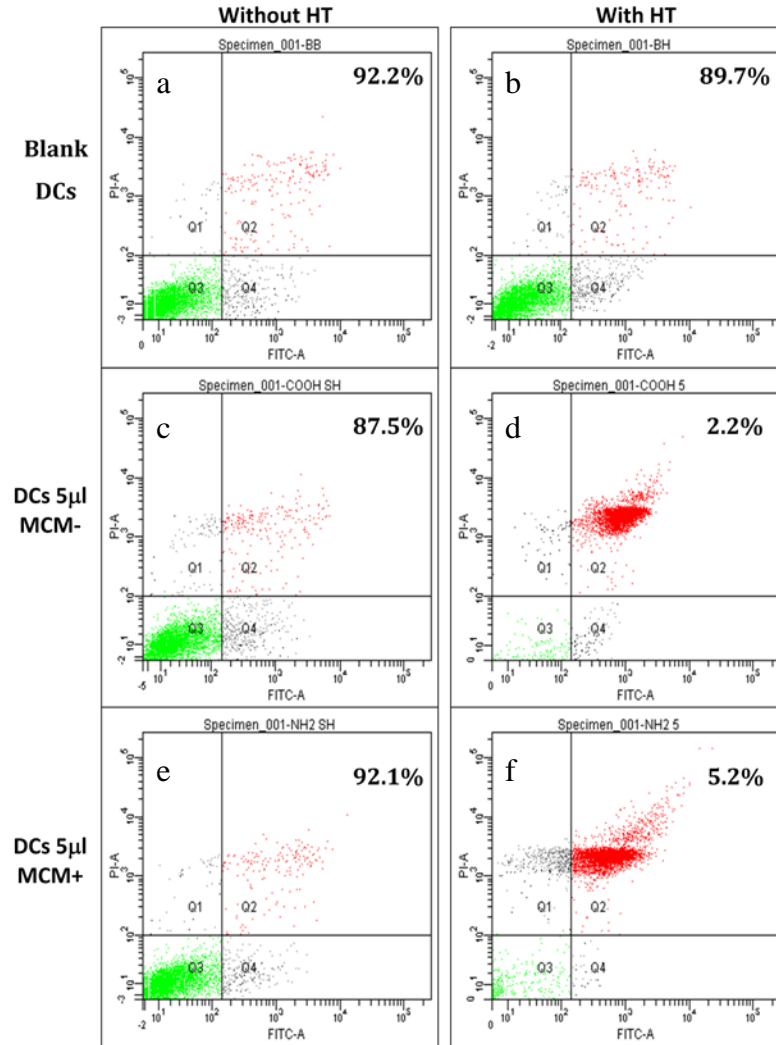


Figure 9: Flow cytometry results for a) unloaded DCs without applied rf field, b) unloaded after applied rf field, c) DCs with MCM-COOH particles without rf field, d) DCs with MCM-COOH particles after rf field, e) co-cultured DCs with MCM-NH₂⁺ particles without rf field, and f) DCs with MCM-NH₂⁺ particles after applied rf field.

Interestingly, the temperature of the cell medium measured by the macroscopic optic sensor remained within the 29-31 °C (see Figure 10), i.e., few degrees above the starting temperature of 26 °C, but in any case well below the values of 43-46 °C needed to trigger temperature-induced apoptosis by hyperthermia. The absence of macroscopic temperature increase together with the level of cell death observed for

samples d) and f) raised the question about a possible intracellular mechanism, different from the temperature increase of the intracellular medium (i.e., magnetic hyperthermia).

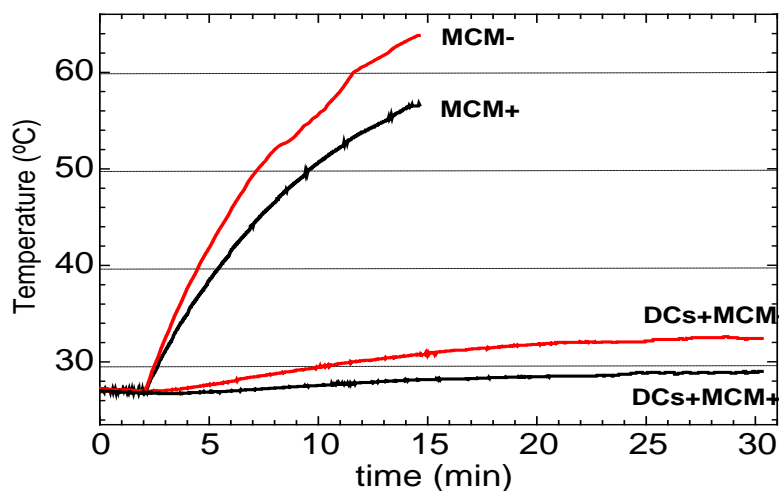


Figure 10: Heating curves for pure colloids (MCM+ and MCM-), and for the cultured DCs during application of ac magnetic fields ($H = 160$ Oe, $f = 260$ kHz).

In a series of comprehensive experiments using CoFe_2O_4 and $\gamma\text{-Fe}_2\text{O}_3$ magnetic NPs, Fortin *et al.* have shown that heating can be achieved with a concentration of 25-30 pg at the intracellular level.[40] In our experiments, we observed a lower amount of NPs uptake (maximum of 5 pg/cell when 30 $\mu\text{l/ml}$ medium of ferrofluid was co-cultured by 12 h) and we believe that this lower amount could be related to different affinities to MNPs among different cell lines. As observed in Figure 10 these amounts of 1-5 pg/cell were not enough to raise the temperature of the whole cell culture when submitted to ac magnetic fields in our thermally-insulated system. We conclude that the temperature increase of the cell culture is not a relevant parameter to induce cell death by AMF in MNP-loaded dendritic cells.

Apoptosis or cellular programmed death is a particular mechanism in which the cells follow a programmed sequence of events to “prepare” their death with

minimal disturbance of the whole population. This phenomenon seems to be present in a wide range of organisms from primitive to higher eukaryotes. An early event that is considered as a marker of this process is the exposition of phosphatidylserine in the external surface of the plasma membrane. The FACS results of Figure 9 indicate that incubation of DCs with annexin (which reveals the presence of phosphatidylserine) and propidium iodide (which reveals damages in the plasma membrane), are both positive only for magnetically charged DCs after application of the AMF (Figs 9 d) and f).

It is important to stress that the experimental protocols were designed to perform the viability analysis immediately after exposure to rf fields. In spite of the short time elapsed between rf exposure and FACS measurement (ca 2 hours), a clear shift of the cell populations along both axes (samples d and f) is observed, showing evidence of late apoptotic or necrotic cells.

The SEM images taken for the cell cultures after AMF application (see Figure 11) showed a clear effect on the membrane integrity after AMF experiments in those DCs loaded with nanoparticles, whereas those cells without loaded NPs retain the complex membrane structure of functional DCs. The short time elapsed and the large damage observed at membrane level supports the hypothesis of a necrotic-like process. The large channels observed in Figure 11(b) suggest that after AMF the cells loose all membrane activity and turned permeable units. The origin of such a dramatic effect attained by a relatively small amount of NPs (ca. 2-5 pg NPs/cell) is not yet clear, but the short time involved (30 min of AMF application and one hour interval before cells were fixed for SEM images) indicates that the process is of physical nature, as opposed to a programmed loss of metabolic activity followed by cell death. In any

case, the release of the power absorbed by the NPs does not yield temperature increase, when measured at the intercellular space (culture medium) by a macroscopic probe. The possibility remains, however, that the temperature of the intracellular medium increases during AMF application, yielding metabolic and/or cytoskeleton damage. This hypothesis has to be checked by a yet undeveloped microscopic, intracellular temperature probe, and work along this direction is currently being done.

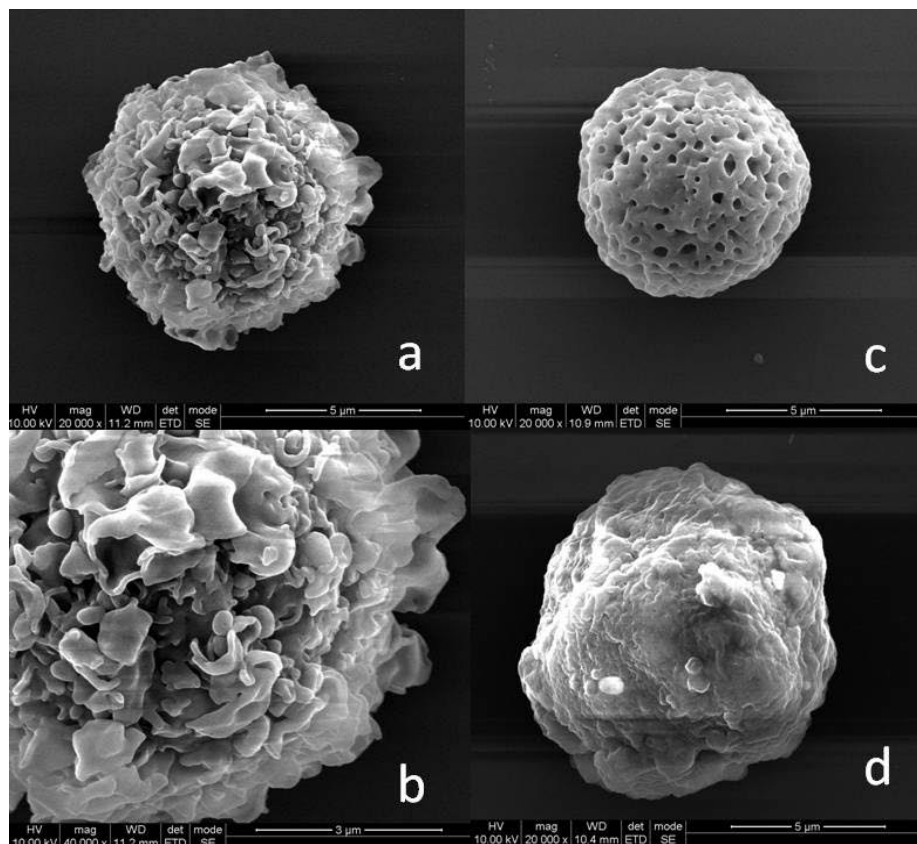


Figure 11: Scanning Electron Microscopy images of DCs after application of AMF for 30 min: a) and b) cells not loaded with MNPs; c) and d) DCs loaded with MNPs. Note the evident loss of membrane structure and ‘shrinking’ of the cells in c) and d). Note also in c) the large channels opened in the membrane.

In spite of the experimental difficulty for measuring intracellular temperature, some theoretical calculations were performed to evaluate the capability of the number of NPs uploaded to release enough energy to damage the subcellular structure. From

the average particle diameter of the NPs measured by TEM images, the number of particles within a single cell ranged from 1×10^4 to 7×10^4 . Assuming the same power absorption than the pure ferrofluid (36-46 W/g, see *Table I*), this amount of MNPs could release a total power of 2×10^{-10} W to the nearest-neighbor organelles. If a short release time of 10 s is considered, the total energy available for local damage could be of the order of 1×10^{10} eV. Compared to typical binding energies per atom in organic molecules ($E_{C-N} = 308$ eV, $E_{C-C} = 348$ eV, $E_{C=C} = 614$ eV), the previous estimation indicates that there is enough energy available to induce bond-breaking on the organic structures surrounding the MNPs.

On the other hand, the fact that these particles are confined within endosomic structures (as observed from TEM images) drastically reduces the contact area with subcellular structures to the endosomic membrane. It seems therefore unlikely that a generalized damage within the cytoplasm can be the origin of the abrupt cell death after AMF application. Instead, these agglomerates observed inside endosomes could be able to disrupt the endosomic membrane during power absorption experiments. Both endosomes and lysosomes are acidic vesicles involved in the endocytic pathway, being the lysosomes the terminal degradation compartment of the phagocytosed material. Therefore, the release of the content of both the endosomes and lysosomes into the cytoplasm would induce several changes in the intracellular medium, leading to cell death in most of the cases.

Although a complete analysis of the actual mechanism at the cellular level would require a study on a variety of markers (such as proteases, caspases, cytokines, etc...), the large fraction of dead cells in this short time allow us to discard a programmed, apoptotic process as the main cause of cell death during magnetic field

application. The precise nature of this mechanism is of crucial importance for future application protocols, since necrosis must always be avoided *in vivo* due to the lethal consequences to the surrounding tissues. In the case of the energy release being the cause of cellular damage, both the application time and power could be regulated down to some value at which only apoptosis is triggered. If rupture of endosomes is the main path to the observed necrotic process, the control of this mechanism appears rather difficult.

Our combined results of a) low cytotoxicity of magnetic MNPs, and b) cell death after application of AMF, suggest that MNPs loaded-DCs could be used as magnetic carriers to tumoral regions, where cellular death induced by an external magnetic field could be used as a therapy against tumor growth.

Conclusion

Based on the described ability of DCs to be loaded with magnetic nanoparticles, they appear as a potentially powerful ‘trojan horse’ system for MNP delivery to specific target sites. Our results showing that MNPs have negligible cytotoxic effects, while keeping the functionality of dendritic cells, support the feasibility of this approach. Bottom line is, subsequent application of an AMF induces cell death, and therefore selective killing of MNP-loaded cells is feasible. The detail of the intracellular mechanism has yet to be understood, but our preliminar results point to an initial disruption of the endosome/lysosome membrane by the MNPs, yielding the release of their content and the consequent cell death.

Future Perspective

In combination with magnetic nanoparticles and hyperthermia treatments, DCs may become a useful tool for many biomedical applications. Since we know the ability of DCs to transdifferentiate into endothelial like cells (ELCs) under proangiogenic conditions and be part of the tumoral vasculature, a combined therapy of NPs-loaded DCs and hyperthermia may constitute an alternative treatment for cancer patients. DCs loaded with magnetic NPs *ex vivo* could be vectorized or injected *in situ* in tumor sites and, under the proangiogenic microenvironment present in the tumor area, DCs might differentiate to ELCs and integrate into the new vasculature. Death of the NPs-loaded cells and therefore, the tumor blood supply, through the exposure to alternate magnetic fields could avoid tumor vessels network formation and create a better prognosis.

Executive Summary

- Dendritic cells were up loaded with magnetic NPs and remained viable after 5 days, retaining their phenotype of immature DCs.
- The amount of magnetic nanoparticles was determined by magnetization measurements to be between 1 to 5 pg/cell.
- By the exposure of the magnetically-loaded DCs to alternating magnetic fields during 30 minutes we were able to induce a 90-95 % cell death.
- Non loaded DCs remained viable after exposure to the alternate magnetic field and their viability is similar to the non exposed DCs to this field.
- The amount of magnetic nanoparticles at the intracellular space was not able to increase the temperature of the culture medium up to the apoptotic values. This situation raises the question about the actual mechanisms during magnetic hyperthermia.
- Clear signals of damage at the cell membrane were observed from SEM images.

Financial & competing interests and disclosure

G.F.G. and M.R.I., along with the University of Zaragoza, have filled patents related to the technology and intellectual property related to magnetic field applicators reported here. G.F.G. and M.R. I. have equity in nB Nanoscale Biomagnetics S.L. The other authors declare that they do not have any affiliations that would lead to conflict of interests.

Acknowledgements

This work was supported by the Ministerio de Ciencia e Innovación (project MAT2008-02764); Diputación General de Aragón (DGA) and IBERCAJA.

References:

1. Vulink A, Radford Kj, Melief C, Hart Dnj: *Dendritic cells in cancer immunotherapy*. In: *Advances in cancer research, vol 99*, (Ed.^(Eds). 363-407 (2008).
2. Banchereau J, Steinman Rm: Dendritic cells and the control of immunity. *Nature* 392(6673), 245-252 (1998).
3. Akira S, Uematsu S, Takeuchi O: Pathogen recognition and innate immunity. *Cell* 124(4), 783-801 (2006).
4. Randolph Gj, Angeli V, Swartz Ma: Dendritic-cell trafficking to lymph nodes through lymphatic vessels. *Nature Reviews Immunology* 5(8), 617-628 (2005).
5. Jin P, Han Th, Ren Jq *et al.*: Molecular signatures of maturing dendritic cells: Implications for testing the quality of dendritic cell therapies. *J. Transl. Med.* 8, 15 (2010).
6. Barakat Ns: Magnetically modulated nanosystems: A unique drug-delivery platform. *Nanomedicine* 4(7), 799-812 (2009).
7. Soenen Sjh, Hodenius M, De Cuyper M: Magnetoliposomes: Versatile innovative nanocolloids for use in biotechnology and biomedicine. *Nanomedicine* 4(2), 177-191 (2009).
8. Riegler J, Wells Ja, Kyrtatos Pg, Price An, Pankhurst Qa, Lythgoe Mf: Targeted magnetic delivery and tracking of cells using a magnetic resonance imaging system. *Biomaterials* 31(20), (2010).
9. Fortina P, Kricka Lj, Surrey S, Grodzinski P: Nanobiotechnology: The promise and reality of new approaches to molecular recognition. *Trends in Biotechnology* 23(4), 168-173 (2005).

10. Goya Gf, Grazu V, Ibarra Mr: Magnetic nanoparticles for cancer therapy. *Current Nanoscience* 4(1), 1-16 (2008).
11. Nie Sm: Understanding and overcoming major barriers in cancer nanomedicine. *Nanomedicine* 5(4), 523-528 (2010).
12. Mohapatra S, Mallick Sk, Maiti Tk, Ghosh Sk, Pramanik P: Synthesis of highly stable folic acid conjugated magnetite nanoparticles for targeting cancer cells. *Nanotechnology* 18(38), (2007).
13. Park Jh, Von Maltzahn G, Zhang Ll *et al.*: Systematic surface engineering of magnetic nanoworms for in vivo tumor targeting. *Small* 5(6), 694-700 (2009).
14. Andersson Lim, Hellman P, Eriksson H: Receptor-mediated endocytosis of particles by peripheral dendritic cells. *Human Immunology* 69(10), 625-633 (2008).
15. Biragyn A, Ruffini Pa, Leifer Ca *et al.*: Toll-like receptor 4-dependent activation of dendritic cells by beta-defensin 2. *Science* 298(5595), 1025-1029 (2002).
16. Molavi L, Mahmud A, Hamdy S *et al.*: Development of a poly(d,l-lactic-co-glycolic acid) nanoparticle formulation of stat3 inhibitor jsi-124: Implication for cancer immunotherapy. *Molecular Pharmaceutics* 7(2), 364-374 (2010).
17. Pujol Bf, Lucibello Fc, Zuzarte M, Lutjens P, Muller R, Havemann K: Dendritic cells derived from peripheral monocytes express endothelial markers and in the presence of angiogenic growth factors differentiate into endothelial-like cells. *European Journal of Cell Biology* 80(1), 99-110 (2001).
18. Harraz M, Jiao Ch, Hanlon Hd, Hartley Rs, Schatteman Gc: Cd34(-) blood-derived human endothelial cell progenitors. *Stem Cells* 19(4), 304-312 (2001).
19. Shirinifard A, Gens Js, Zaitlen Bl, Poplawski Nj, Swat M, Glazier Ja: 3d multi-cell simulation of tumor growth and angiogenesis. *Plos One* 4(10), (2009).
20. Reyes M, Dudek A, Jahagirdar B, Koodie L, Marker Ph, Verfaillie Cm: Origin of endothelial progenitors in human postnatal bone marrow. *Journal of Clinical Investigation* 109(3), 337-346 (2002).
21. Ikpeazu C, Davidson Mk, Halteman D, Goodman Sa, Browning Pj, Brandt Sj: Donor origin of circulating endothelial progenitors after allogeneic bone marrow transplantation. *Biology of Blood and Marrow Transplantation* 6(3A), 301-308 (2000).
22. Basic specifications from the provider includes: Hydrodynamic size: 250 nm; np concentration: 10 mg/ml (4.9×10^{11} mnps/ml); polydispersity index < 0.2; ms ($h = 1 t$) = 67 emu/g. . (2009).
23. Conejo-Garcia Jr, Buckanovich Rj, Benencia F *et al.*: Vascular leukocytes contribute to tumor vascularization. *Blood* 105(2), 679-681 (2005).
24. Lutsiak Mec, Robinson Dr, Coester C, Kwon Gs, Samuel J: Analysis of poly(d,l-lactic-co-glycolic acid) nanosphere uptake by human dendritic cells and macrophages in vitro. *Pharmaceutical Research* 19(10), 1480-1487 (2002).
25. Coester C, Nayyar P, Samuel J: In vitro uptake of gelatin nanoparticles by murine dendritic cells and their intracellular localisation. *European Journal of Pharmaceutics and Biopharmaceutics* 62(3), 306-314 (2006).
26. Macpherson G, Milling S, Yrlid U, Cousins L, Turnbull E, Huang Fp: Uptake of antigens from the intestine by dendritic cells. *Oral Tolerance: New Insights and Prospects for Clinical Application* 1029, 75-82 (2004).

27. Sabado Rl, Babcock E, Kavanagh Dg *et al.*: Pathways utilized by dendritic cells for binding, uptake, processing and presentation of antigens derived from hiv-1. *European Journal of Immunology* 37(7), 1752-1763 (2007).
28. Goya Gf, Marcos-Campos I, Fernandez-Pacheco R *et al.*: Dendritic cell uptake of iron-based magnetic nanoparticles. *Cell Biology International* 32(8), 1001-1005 (2008).
29. Kalambur Vs, Longmire Ek, Bischof Jc: Cellular level loading and heating of superparamagnetic iron oxide nanoparticles. *Langmuir* 23, 12329-12336 (2007).
30. Goya Gf, Lima E, Arelaro Ad *et al.*: Magnetic hyperthermia with fe₃o₄ nanoparticles: The influence of particle size on energy absorption. *Ieee Transactions on Magnetism* 44(11), 4444-4447 (2008).
31. Goya Gf, Berquo Ts, Fonseca Fc, Morales Mp: Static and dynamic magnetic properties of spherical magnetite nanoparticles. *Journal of Applied Physics* 94(5), 3520-3528 (2003).
32. Posfai M, Moskowitz Bm, Arato B *et al.*: Properties of intracellular magnetite crystals produced by desulfovibrio magneticus strain rs-1. *Earth and Planetary Science Letters* 249(3-4), 444-455 (2006).
33. Verges Ma, Costo R, Roca Ag *et al.*: Uniform and water stable magnetite nanoparticles with diameters around the monodomain-multidomain limit. *Journal of Physics D-Applied Physics* 41(13), (2008).
34. Hamoir J, Nemmar A, Halloy D *et al.*: Effect of polystyrene particles on lung microvascular permeability in isolated perfused rabbit lungs: Role of size and surface properties. *Toxicology and Applied Pharmacology* 190(3), 278-285 (2003).
35. Panyam J, Zhou Wz, Prabha S, Sahoo Sk, Labhasetwar V: Rapid endo-lysosomal escape of poly(dl-lactide-co-glycolide) nanoparticles: Implications for drug and gene delivery. *Faseb Journal* 16(10), (2002).
36. Wang J, Sun Rh, Zhang N *et al.*: Multi-walled carbon nanotubes do not impair immune functions of dendritic cells. *Carbon* 47(7), 1752-1760 (2009).
37. Levy M, Wilhelm C, Siaugue Jm, Horner O, Bacri Jc, Gazeau F: *Magnetically induced hyperthermia: Size-dependent heating power of gamma-fe₂o₃ nanoparticles*. In: *11th International Conference on Magnetic Fluids*. Kosice, SLOVAKIA 2007.
38. Gonzalez-Fernandez Ma, Torres Te, Andres-Verges M *et al.*: Magnetic nanoparticles for power absorption: Optimizing size, shape and magnetic properties. *Journal of Solid State Chemistry* 182, 6 (2009).
39. Natividad E, Castro M, Mediano A: Accurate measurement of the specific absorption rate using a suitable adiabatic magnetothermal setup. *Applied Physics Letters* 92(9), (2008).
40. Fortin Jp, Gazeau F, Wilhelm C: Intracellular heating of living cells through neel relaxation of magnetic nanoparticles. *European Biophysics Journal with Biophysics Letters* 37(2), 223-228 (2008).

WEBSITE

- [101] “Magforce nanotechnologies ag receives european regulatory approval for its Nanocancer® therapy.” <http://www.magforce.de/english/press/press-releases/pm/article-1277714705>, (2010).

[102] Micromod Partikeltechnologie GmbH. Product labeling was: nanomag®-D, nanomag®-CLD, and nanomag®-D-spio. Company website: <http://www.micromod.de> .